

Structural Insights into the Asymmetric Effects of Zinc-Ligand Cysteine Mutations in the Novel Zinc Ribbon Domain of Human TFIIE α for Transcription

Masahiko Okuda^{1,2}, Aki Tanaka^{3,4}, Fumio Hanaoka^{3,5}, Yoshiaki Ohkuma^{3,*} and Yoshifumi Nishimura^{1,†}

¹International Graduate School of Arts and Sciences, Yokohama City University, 1-7-29, Suehiro-cho, Tsurumi-ku, Yokohama 230-0045; ²Kihara Memorial Yokohama Foundation for the Advancement of Life Sciences, 1-7-29, Suehiro-cho, Tsurumi-ku, Yokohama 230-0045; ³Graduate School of Frontier Biosciences, Osaka University, 1-3 Yamada-oka, Suita, Osaka 565-0871; ⁴Graduate School of Pharmaceutical Sciences, Osaka University, 1-6 Yamada-oka, Suita, Osaka 565-0871; and ⁵Cellular Physiology Laboratory, RIKEN, 2-1 Hirosawa, Wako, Saitama 351-0198

Received May 7, 2005; accepted July 21, 2005

The large subunit of TFIIE (TFIIE α) has a highly conserved zinc ribbon domain, which is essential for transcription. Recently, we determined the solution structure of this domain to be that of a novel zinc finger motif [Okuda *et al.* (2004) *J. Biol. Chem.* 279, 51395–51403]. On examination of the functions of four cysteine mutants of TFIIE α , in which each of four zinc-liganded cysteines was replaced by alanine, we found an interesting functional asymmetry; on a supercoiled template, the two C-terminal mutants did not show any transcriptional activity, however, the two N-terminal mutants retained about 20% activity. Furthermore, these two pairs of mutants showed distinct binding abilities as to several general transcription factors. To obtain structural insights into the asymmetry, here we have analyzed the structures of the four cysteine mutants of the zinc ribbon domain by CD and NMR. All four mutants possessed a characteristic partially folded structure coordinating with a zinc atom, despite the imperfect set of cysteine-ligands. However, they equilibrated with several structures including the random coil structure. Unexpectedly, the two N-terminal mutants mainly equilibrated with the random coil structure, while the two C-terminal ones mainly equilibrated with folded structures. The characteristic structure formation of each mutant was reversible, which totally depended on the zinc binding.

Key words: CD, NMR, TFIIE, transcription, Zn²⁺-binding.

Abbreviations: 6His, six histidine-tag; CTD, C-terminal domain of the largest subunit of Pol II; HSQC, heteronuclear single quantum correlation; hTFIIE α c, core domain of human TFIIE α ; NOE, nuclear Overhauser effect; PIC, preinitiation complex; Pol II, RNA polymerase II.

Initiation of the transcription of eukaryotic protein coding genes requires RNA polymerase II (Pol II) and five general transcription factors, TFIIB, TFIID, TFIIE, TFIIIF, and TFIIH (1, 2). Promoter DNA-binding of the TATA box-binding protein (TBP), a subunit of TFIID, triggers this initiation. It is followed by stepwise assembly of TFIIB, Pol II/TFIIIF, TFIIE, and TFIIH, and then a preinitiation complex (PIC) is formed on the promoter containing the transcription initiation site. During PIC formation, TFIIE interacts with various general transcription factors, Pol II and promoter DNA, and recruits TFIIH to the PIC (3). TFIIE also plays direct roles in the transition from initiation to elongation via promoter melting and promoter clearance by regulating the enzymatic activities of TFIIH; those of serine-kinase of the C-terminal domain (CTD)

of the largest subunit of Pol II, DNA-dependent ATPase, and DNA helicase (4–8).

Human TFIIE (hTFIIE) is a heterotetramer consisting of two α (hTFIIE α ; 57 kDa) and two β (hTFIIE β ; 34 kDa) subunits (9–12). While its functions have been studied well, little is known about its structure (13–16). Recently, we determined the solution structure of the core domain of hTFIIE α (hTFIIE α c) (17). Although the N-terminal and C-terminal regions were flexible, the residual middle region comprised a compact structure, consisting of five β -strands and one α -helix (Fig. 1). This structure can be classified as a novel zinc finger, because of no similarity with any other zinc finger structures determined so far. However, its Zn²⁺-binding site formed by two turns (t1, t2) was quite similar to the sites of zinc ribbon structures (18–24). Two pairs of cysteine residues on each of the two turns coordinated with Zn²⁺. These two turns were symmetrical: the S γ atom of the first Zn²⁺-ligand, C129, formed bifurcated hydrogen bonds with the amide protons of V131 and the second Zn²⁺-ligand, C132, behind the second and third residues on the first turn, t1. The same hydrogen bond patterns were observed for the second turn,

*Present address: Department of Biological Chemistry, Faculty of Pharmaceutical Sciences, Toyama Medical and Pharmaceutical University, 2630 Sugitani, Toyama 930-0194.

†To whom correspondence should be addressed. Tel: +81-45-508-7216, Fax: +81-45-508-7362, E-mail: nishimura@tsurumi.yokohama-cu.ac.jp

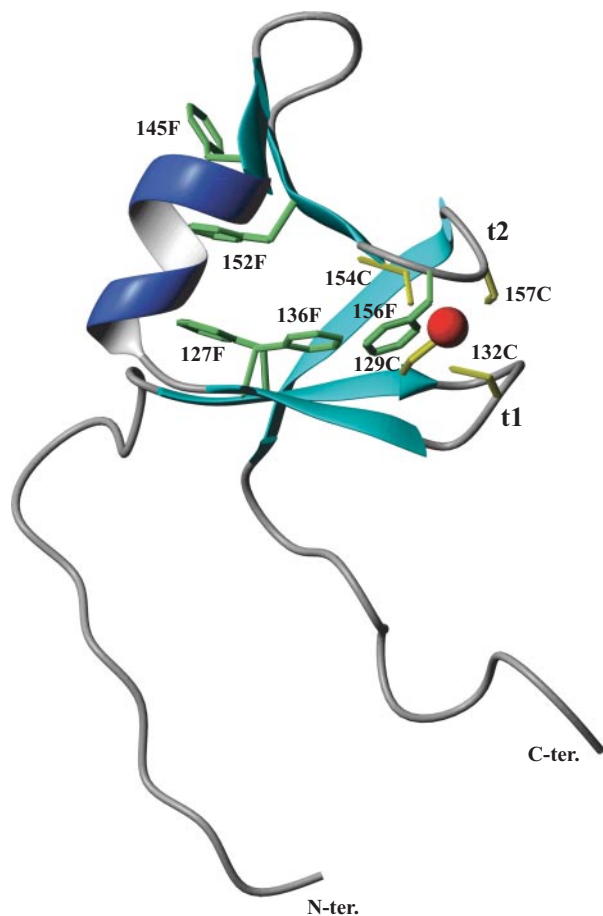


Fig. 1. The hTFIIIE α structure. Solution structure of hTFIIIE α (17). The two turns comprising the Zn $^{2+}$ -binding site are indicated by t1 and t2. Zn $^{2+}$ is shown as a red sphere. The four Zn $^{2+}$ -coordinating cysteine residues are shown in yellow. The five phenylalanine residues are shown in green. This figure was made using the program MOLMOL (35). The atomic coordinates have been deposited in the Protein Data Bank, Research Collaboratory for Structural Bioinformatics, Rutgers University, New Brunswick, NJ (<http://www.rcsb.org/>) under the accession code 1VD4.

t2. That is, there were bifurcated hydrogen bonds between the S γ atom of the third Zn $^{2+}$ -ligand, C154, and the amide protons of F156 and the fourth Zn $^{2+}$ -ligand, C157. These hydrogen bonds enhanced the stability of the Zn $^{2+}$ -binding site. In order to reveal the function of hTFIIIE α , we created four cysteine point mutants, alanines being substituted for cysteines, at the Zn $^{2+}$ -binding site (C129A, C132A, C154A, and C157A), and performed mutation analysis for basal transcription activity (17). The results showed an interesting asymmetry of the Zn $^{2+}$ -ligands for the transcription activity. None of the cysteine mutants showed any transcription activity on a linearized DNA template of the adenovirus 2 major late promoter, however, on a supercoiled template, the two N-terminal cysteine mutants, C129A and C132A, retained about 20% transcription activity, contrary to the two C-terminal cysteine mutants, C154A and C157A, which possessed no transcription activity. GST-pull down assaying of TFIIIE α with TFIIIE β as well as other general transcription factors showed that C129A and C132A bound more strongly to TFIIIE β compared with C154A and C157A,

rather than the wild type, whereas C154 exhibited reduced and C157A absolutely no binding ability as to the XPB subunit of TFIIH. Here, we obtained structural insights into the asymmetry of the Zn $^{2+}$ -ligands of hTFIIIE α by CD and NMR.

MATERIALS AND METHODS

Purification of hTFIIIE α Mutants—Construction of the expression plasmids for the wild type and mutants of hTFIIIE α , and purification of the wild type were described previously (17). Each hTFIIIE α point mutant plasmid was transformed into *E. coli* BL21(DE3)pLysS (Novagen). The cells were grown at 37°C in M9 minimal medium containing [15 N] ammonium chloride. A six histidine-tag (6His)-hTFIIIE α point mutant was then induced by the addition of 1 mM isopropyl- β -D-thiogalactopyranoside (IPTG). Sixty μ M ZnCl $_2$ was added to the medium at the same time. After 6 h growth the cells were harvested. The cell pellet was resuspended in buffer A [20 mM Tris-HCl (pH 7.0), 10% (v/v) glycerol, 30 μ M ZnCl $_2$, 5 mM β -mercaptoethanol, 1 mM phenylethylsulfonyl fluoride (PMSF), 1 mM benzamidine] containing 100 mM NaCl (BA100). The cells were lysed by sonication and centrifuged, and then the supernatant was loaded onto a Ni-nitrilotriacetic acid (NTA)-agarose (Qiagen) column equilibrated with BA100 containing 20 mM imidazole-HCl. The sample was eluted with a linear gradient of 20 to 400 mM imidazole-HCl. The peak fractions were pooled and diluted to approximately 2-fold volume with a buffer (BA0, 100 mM NaCl-free BA100), and then applied to a Q-Sepharose column (Amersham Pharmacia Biotech) equilibrated with BA0. The sample was eluted with a linear gradient of 0 to 1 M NaCl. The peak fractions were pooled and the buffer was changed to 50 mM Tris-HCl (pH 8.0), 30 μ M ZnCl $_2$, 5 mM β -mercaptoethanol, 2.5 mM CaCl $_2$ containing 150 mM NaCl. The sample was digested with thrombin for 16 h at 25°C to remove the 6His-tag, concentrated using Centrprep (Amicon), and then applied to a Superdex30 column (Amersham Pharmacia Biotech) equilibrated with a buffer [20 mM potassium phosphate (pH 6.0), 30 μ M ZnCl $_2$, 5 mM 1,4-dithiothreitol (DTT)] containing 50 mM NaCl. The final fractions were used for analyses.

CD Spectroscopy—Fifteen micromolar aliquots of the wild type and mutant hTFIIIE α were dissolved in a buffer [10 mM potassium phosphate (pH 6.0), 30 μ M ZnCl $_2$, 1.0 mM DTT]. CD spectra were obtained at 25°C on a Jasco J-720W spectropolarimeter with a 1 mm path-length cell. Each spectrum was the average of 16 scans over the wavelength range of 185–260 nm. The secondary structure was analyzed according to the method of Yang *et al.* (25).

NMR Spectroscopy—The protein concentration for 2D 1 H NOESY experiments was 0.5 mM in a buffer [20 mM potassium phosphate (pH 6.0), 30 μ M ZnCl $_2$, 5.0 mM deuterated DTT, 50 mM NaCl] in 99.9% D $_2$ O. All NMR experiments were carried out at 27°C on a Bruker Avance 600 spectrometer. Spectra were processed using NMRPipe (26), and analyzed using the programs PIPP, CAPP, STAPP (27), and NMRView (28).

EDTA Titration—EDTA was added in 0.5 mM increments up to 2.0 mM to 1 mM aliquots of the 15 N-labeled wild type and mutant hTFIIIE α in a buffer [20 mM potassium phosphate (pH 6.0), 30 μ M ZnCl $_2$, 5.0 mM

deuterated DTT, containing 50 mM NaCl] in 90% H₂O/10% D₂O. ¹H-¹⁵N HSQC spectra were taken after each EDTA addition.

ZnCl₂ Titration—Each sample used in the EDTA titration experiments was dialyzed against a buffer [20 mM potassium phosphate (pH 6.0), 5.0 mM DTT, containing 50 mM NaCl] to remove EDTA and ZnCl₂. After removing the precipitate generated during the dialysis

by centrifugation, the supernatant was concentrated using Centricon (Amicon) up to 0.6 mM. ZnCl₂ was added in 0.3 mM increments up to 1.2 mM to 0.6 mM aliquots of the ¹⁵N-labeled wild type and mutant hTFIIIE α c in a buffer [20 mM potassium phosphate (pH 6.0), 5.0 mM deuterated DTT, containing 50 mM NaCl] in 90% H₂O/10% D₂O. ¹H-¹⁵N HSQC spectra were taken after each ZnCl₂ addition.

RESULTS

All Zn²⁺-Ligand Mutants Have Characteristic Partially Folded Structures—CD spectra were measured for the wild type and mutants of hTFIIIE α c to examine their secondary structures. Figure 2 shows that the spectra of C129A and C132A are similar to each other, and C154A and C157A also resemble each other in their spectra. Since hTFIIIE α c is a small domain with little regular secondary structure, accurate calculation of the secondary structure content from a CD spectrum is difficult. So, we estimated relative ratios of β sheet to random coil. Given that the ratio for the wild type is 1.00, ones of 0.41 for C129A, 0.47 for C132A, 0.69 for C154A, and 0.65 for C157A were calculated. This suggests that the C-terminal mutants, C154A and C157A, contain a larger quantity of folded structure than the N-terminal ones, C129A and C132A.

Next, 2D ¹H NOESY NMR spectra were recorded (Fig. 3). To check NOE signals between the aromatic and aliphatic side-chains clearly, samples were measured in D₂O. hTFIIIE α c has no tyrosine or tryptophan residues, but has

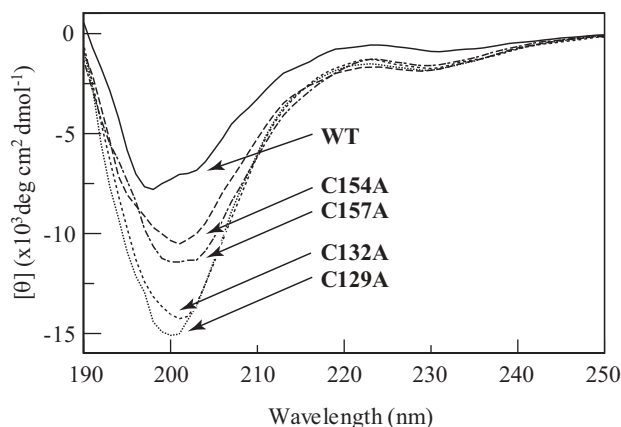


Fig. 2. Far UV CD spectra of the wild type and Zn²⁺-ligand mutated hTFIIIE α c. CD spectra were measured using 15 μ M aliquots of the wild type (WT) and point mutant, C129A, C132A, C154A and C157A, hTFIIIE α c in a buffer [10 mM potassium phosphate (pH 6.0), 30 μ M ZnCl₂, 1.0 mM DTT] at 25°C.

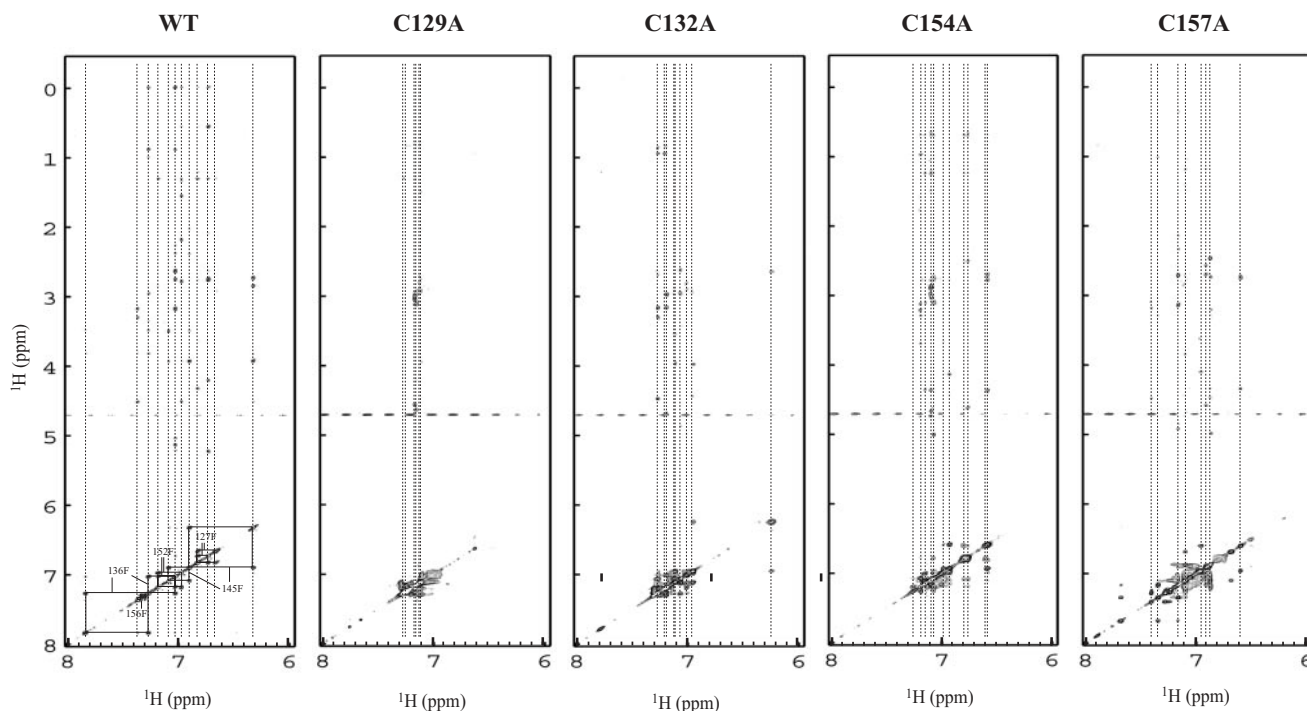
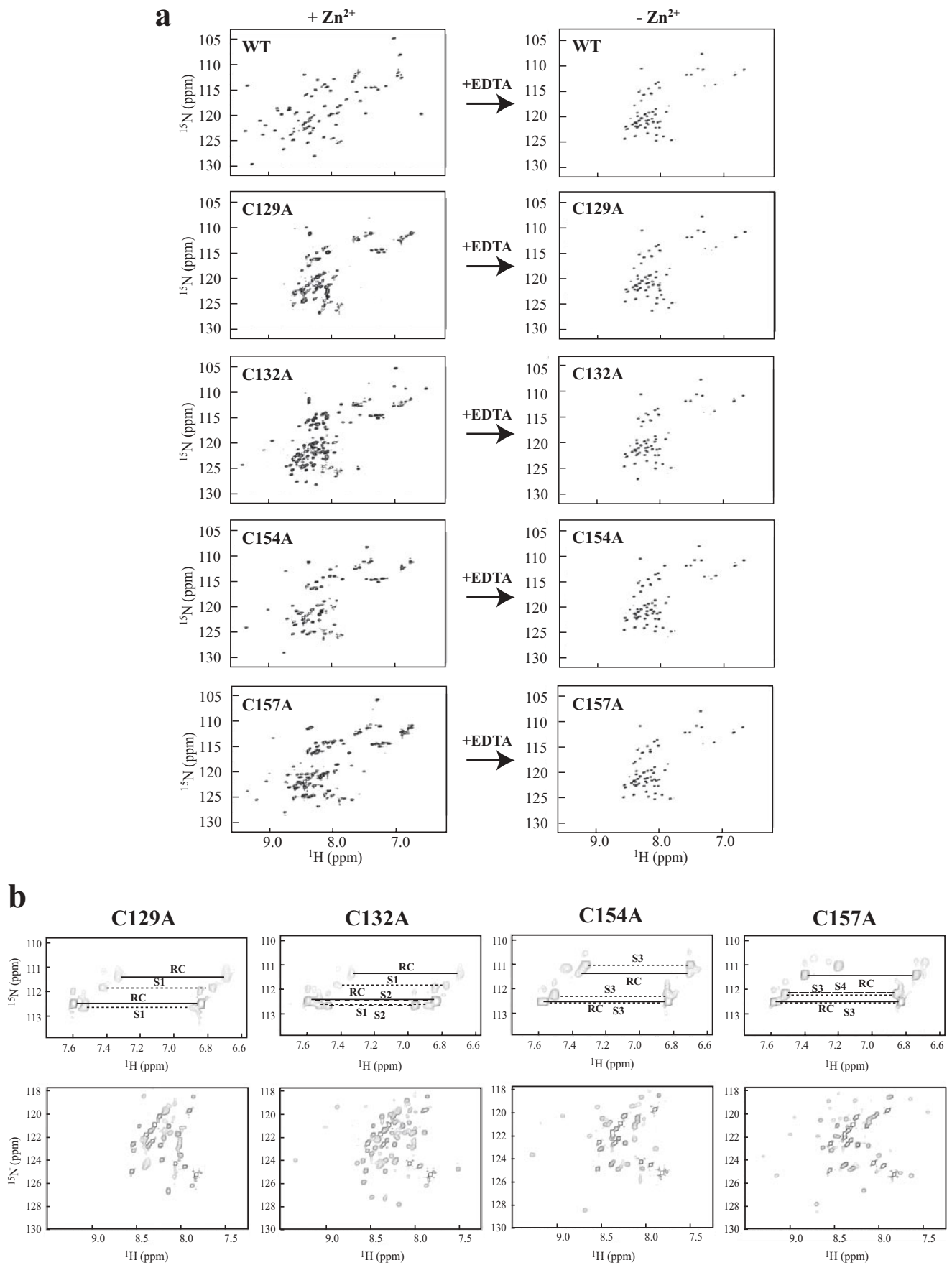


Fig. 3. 2D ¹H NOESY spectra of the wild type and Zn²⁺-ligand mutated hTFIIIE α c. 2D ¹H NOESY experiments were performed using 220 μ l aliquots of 0.5 mM wild type (WT) and point mutant, C129A, C132A, C154A and C157A, hTFIIIE α c in a buffer [20 mM potassium phosphate (pH 6.0), 30 μ M ZnCl₂, 5 mM deuterated DTT, 50 mM NaCl] in 99.9% D₂O at 27°C. The downfield portions of the spectra are shown. In the spectrum of the wild type, the assigned aromatic side-chain signals are linked by a solid line. NOE signals between the aromatic and aliphatic side-chains are linked by a broken line.



five highly conserved phenylalanine ones. They are piled up on each other (Fig. 1). This aromatic-aromatic interaction network contributes significantly to the structure construction (17). Aromatic side-chain signals in the spectrum of the wild type are well dispersed, and many NOE signals between the aromatic-aliphatic and also the aromatic-aromatic side-chains are observed. On the contrary, aromatic signals of C129A are degenerated around 6.9 to 7.3 ppm, suggesting striking structure disruption. Similar signal degeneration is found in the spectrum of C132A, though fine dispersed signals are observed upfield at 6.24 ppm and 6.95 ppm. In the spectrum of C154A, several aromatic signals are dispersed upfield, compared to those of C129A. In addition, some downfield dispersed signals are found in the spectrum of C157A. For all mutants a common observation was that many broadening signals were detected. This means that their structures are heterogeneous and chemically exchanging, or aggregated. The retention times of all mutants on size-exclusion chromatography were a little lower than that of the wild type, but they did not appear to be polymers of unknown molecular size on NMR. Although the NOE signals of all mutants, in particular C129A, are far fewer than those of the wild type, they suggest local structures in these mutants.

Asymmetry of Zn²⁺-Ligand Mutations for the Structure—The inability to assign signals unambiguously makes it hard for us to discuss the partially folded structures of the mutants in detail. To overcome this difficulty and to characterize the structures, we carefully compared the spectra of the mutants and wild type. Besides, we were very interested in the Zn²⁺-binding ability of all point mutants, which lack one of four cysteine residues. Therefore, we carried out EDTA titration experiments for the wild type and mutants of hTFIIE α c, monitoring NMR ¹H-¹⁵N HSQC. Figure 4 shows that by adding an equivalent molar amount of EDTA to the protein solutions, the signal dispersion in the spectra of all four mutants and the wild type completely vanished, indicating that all were unfolded into the random coil structure. Spectra before and after adding a 2-fold excess of EDTA are shown in Fig. 4a. In the C129A spectrum before the addition of EDTA, most, but not all, signals coincided with the signals of the random coil structure obtained on the removal of Zn²⁺. hTFIIE α c has two asparagine and one glutamine residue, so three pairs of amino group signals are observable in the ¹H-¹⁵N HSQC spectrum. While the C129A spectrum shows four pairs, of which two pairs coincided with the signals of the random coil structure and the other two pairs are distinct from the signals of the wild type (Fig. 4b), suggesting that in C129A the random coil structure is predominant but is likely to be equilibrated with a

small quantity of a folded structure coordinating with Zn²⁺. Hereafter this presumed folded structure is referred to as S1. In the spectrum of C132A, 104 main-chain signals are observed contrary to 57 signals in the wild type spectrum (Fig. 4a). The C132A spectrum is similar to the C129A spectrum, showing a number of identical signals, intensive signals originating from the random coil structure and also the corresponding signals for S1 (Fig. 4b). Beside these identical signals, C132A exhibits many different dispersed signals, suggesting a different characteristic folded structure coordinating with Zn²⁺, which is designated as S2. The amino groups of asparagine and glutamine residues in C132A reflected six pairs; two pairs are identical to the pairs of S1 found in C129A and two other pairs coincided with the pairs originating from the random coil structure. The remaining two pairs are likely to correspond to the signals of S2. C132A likely equilibrates in three structures: a very similar structure to S1, a characteristic folded structure, S2, and the random coil structure as a main component.

The spectra of C154A and C157A are also similar to each other, including more dispersed signals and fewer intense signals compared to the C129A and C132A spectra (Fig. 4a). Figure 4b shows that for the amino groups of asparagine and glutamine residues, five pairs are observed in the C154A spectrum. Two pairs originate from the random coil structure and the other pairs seem to be caused by a Zn²⁺-coordinating folded structure designated as S3. C154A is likely to equilibrate between the presumed folded structure, S3 and the random coil structure, though the random coil structure is less dominant than in C129A and C132A. This is consistent with the secondary structure estimation by CD. The HSQC spectrum of C157A also shows five pairs of amino groups; two pairs originated from the random coil structure, however, of the other three pairs two are found to be same as the pairs corresponding to S3 in C154A (Fig. 4b). As for the main-chain, 77 signals are observed in Figure 4a. Most of these signals seem to originate from a similar structure to S3 and the random coil structure, but some different signals from these two structures are also observed, suggesting another different Zn²⁺-coordinating structure designated as S4 (Fig. 4b). C157A likely equilibrates in three structures; a similar structure to S3 found in C154, the other folded structure, S4 and the random coil structure. After the EDTA titration experiments, we reciprocally performed ZnCl₂ titration experiments for samples dialyzed to remove EDTA and Zn²⁺. The addition of ZnCl₂ restored the dispersed signals and the addition of an equivalent amount of ZnCl₂ led to the same spectra as those before EDTA addition. This indicates the reversibility of the Zn²⁺-dependent structure formation in the mutants as well as in the wild type (data not shown).

Fig. 4. EDTA titration experiments for the wild type and Zn²⁺-ligand mutated hTFIIE α c. (a) ¹H-¹⁵N HSQC spectra were acquired using 220 μ l aliquots of 0.5 mM ¹⁵N-labeled wild type (WT) and point mutant, C129A, C132A, C154A and C157A, hTFIIE α c in a buffer [20 mM potassium phosphate (pH 6.0), 30 μ M ZnCl₂, 5 mM deuterated DTT, 50 mM NaCl] in 90% H₂O/10% D₂O at 27°C. Spectra before (+Zn²⁺) and after (-Zn²⁺) adding a 2-fold excess of EDTA to the samples are shown on the left and right sides, respectively. (b) Structural similarity between mutants. Side-chain signals of

asparagine and glutamine residues, and dispersed main-chain signals in the ¹H-¹⁵N HSQC spectra of the mutants are shown in the upper and lower panels, respectively. In the upper panels, a pair of signals is linked by a line. RC: signals coinciding with those in the spectrum after the addition of EDTA (corresponding to the random coil structure). S1: common signals observed in the spectra of both C129A and C132A. S2: signals observed in the only spectrum of C132A. S3: common signal between C154A and C157A. S4: in only C157A.

DISCUSSION

The significance of TFIIEx α for TFIIIE functions has been proved by various evidence obtained in mutation works (13, 17, 29–33). Our previous studies also revealed that Zn²⁺-ligand cysteine mutants, *i.e.*, C129A, C132A, C154A and C157A, had dramatically reduced or absolutely no transcription activity, suggesting the importance of structural integrity of TFIIEx α (17). More noticeable is that the two N-terminal cysteine mutants, C129A and C132A, retain about 20% transcription activity on transcription with the supercoiled template, and the two N-terminal and two C-terminal cysteine mutants show different binding abilities as to TFIIIF β and the XPB subunit of TFIIH. Similar asymmetry was found on point mutant analysis of yeast TFIIEx α (29). Since removal of Zn²⁺ from TFIIEx α entirely disrupts its structure and results in the random coil structure, we are interested in the relationship between structures and residual transcription activity of mutants, and the asymmetric effects of the two N-terminal and two C-terminal cysteine mutants on the transcription activity and binding ability. To elucidate the functional asymmetry of cysteine mutants based on the structure, we have analyzed individual structures of cysteine mutants of hTFIIEx α in comparison with the wild type. Here we distinguish the characteristic folded structures observed in the ¹H-¹⁵N HSQC spectra of mutants as S1, S2, S3 and S4. However, one should pay attention to such structural distinction. Because their NMR signals could not be assigned unambiguously due to line broadening, we had to rely on only the chemical shift coincidence to distinguish their structures. So our structural distinction might involve some ambiguity. Nevertheless, the results clearly show that the structures of the two N-terminal mutants, C129A and C132A, are similar to each other with respect to the extent of NMR signals derived from the random coil structure and chemical shift agreements of the partially folded structures, being distinct from the structures of the wild type and the two C-terminal mutants, C154A and C157A. This is true for the two C-terminal mutants. Although this structural similarity pairing can explain their asymmetric effects on the transcription activity and binding ability, the structures of C129A and C132A are almost denatured, a small quantity of one or two characteristic folded structures, S1 and S2, being retained, and C154A and C157A retain one or two characteristic folded structures, S3 and S4, equilibrated with a small quantity of the random coil structure. All of the presumed characteristic folded structures of S1, S2, S3 and S4 coordinate with Zn²⁺ and are entirely distinct from the native structure of the hTFIIEx α wild type as judged from their NOESY and ¹H-¹⁵N HSQC spectra. At first we assumed that the residual transcriptional activity of the two N-terminal mutants, C129A and C132A, on transcription on the supercoiled template was caused by a native-like folded structure partly existing in the mutants, whereas the lack of transcription activity of the two C-terminal mutants, C154A and C157A, was due to the completely disrupted random coil structure. Thus, the structures of the Zn²⁺-ligand mutants of hTFIIEx α , as revealed by CD and NMR, were not anticipated by us. One possible explanation is that the denatured structure of hTFIIEx α could be folded partially into a native-like structure during transcription

on the supercoiled template; C129A and C132A partially retain the transcription activity. In contrast, C154A and C157A possess a characteristic incorrect folded structure such as S3, different from the native structure, which might inhibit transcription initiation on the supercoiled template. If this were true, the wild type TFIIIE may exhibit some weak activity in the absence of Zn²⁺. However, to examine this idea is difficult, because some factors that are necessary for transcription activity coordinate with Zn²⁺. Even if we can prepare the wild type TFIIIE with Zn²⁺ removed, coordination with Zn²⁺ from other factors may occur. Even C129A and C132A lost all transcription activities on the linear template, for which the transition from initiation to elongation for both TFIIIE and TFIIH is necessary. Therefore the structural integrity of hTFIIEx α is absolutely required for TFIIIE functions, especially in the transition step, which needs complicated interplay between TFIIIE, TFIIIF, TFIIH and Pol II. The changes in the binding ability of the cysteine mutants as to TFIIIF β and the XPB subunit of TFIIH we observed in our previous studies suggest the potential of TFIIEx α to affect the interaction among TFIIIE, TFIIIF and TFIIH (17). Hence, we propose that TFIIEx α regulates positional changes of TFIIIF and TFIIH by altering the relative configuration of the intramolecular domains of TFIIIE.

The Zn²⁺-binding site of hTFIIEx α is similar to the corresponding sites of zinc ribbon structures (18–24). However, the dependence on the Zn²⁺-binding for structure maintenance seems to be different. A recent study on the zinc ribbon structure of the N-terminal domain of human TFIIIB revealed that the overall backbone fold of the Zn²⁺-free state was essentially identical to that of the Zn²⁺-bound one (34). In the case of hTFIIEx α , the absence of Zn²⁺ gives it the random coil structure. Whether Zn²⁺-free TFIIIB is functional remains unknown.

The structural features of the mutants revealed in this work will allow interpretation of the results of various mutation analyses of the Zn²⁺-binding site of TFIIIE (13, 17, 29–33), however, we need further study to determine the exact role of the zinc ribbon structure of TFIIEx α in transcription.

This work was supported by a grant for Collaborative of Regional Entities for the Advancement of Technological Excellence (CREATE) from the Japan Science and Technology Agency, by the Project on Protein 3000, Transcription and Translation, and by Grants-in-Aid for Scientific Research from the Ministry of Education, Culture, Sports, Science and Technology.

REFERENCES

1. Roeder, R.G. (1996) The role of general initiation factors in transcription by RNA polymerase II. *Trends Biochem. Sci.* **21**, 327–335
2. Orphanides, G., Lagrange, T., and Reinberg, D. (1996) The general transcription factors of RNA polymerase II. *Genes Dev.* **10**, 2657–2683
3. Ohkuma, Y. (1997) Multiple functions of general transcription factors TFIIIE and TFIIH in transcription: possible points of regulation by trans-acting factors. *J. Biochem.* **122**, 481–489
4. Lu, H., Zawel, L., Fisher, L., Egly, J.-M., and Reinberg, D. (1992) Human general transcription factor IIIH phosphorylates

- the C-terminal domain of RNA polymerase II. *Nature* **358**, 641–645
5. Ohkuma, Y., and Roeder, R.G. (1994) Regulation of TFIIF ATPase and kinase activities by TFIIE during active initiation complex formation. *Nature* **368**, 160–163
 6. Dvir, A., K. Garrett, P., Chalut, C., Egly, J.-M., Conaway, J.W., and Conaway, R.C. (1996) A role for ATP and TFIIF in activation of the RNA polymerase II preinitiation complex prior to transcription initiation. *J. Biol. Chem.* **271**, 7245–7248
 7. Douziech, M., Coin, F., Chipoulet, J.-M., Arai, Y., Ohkuma, Y., Egly, J.-M., and Coulombe, B. (2000) Mechanism of promoter melting by the xeroderma pigmentosum complementation group B helicase of transcription factor IIF revealed by protein-DNA photo-cross-linking. *Mol. Cell. Biol.* **20**, 8168–8177
 8. Drapkin, R., Reardon, J.T., Ansari, A., Huang, J.C., Zawel, L., Ahn, K., Sancar, A., and Reinberg, D. (1994) Dual role of TFIIF in DNA excision repair and in transcription by RNA polymerase II. *Nature* **368**, 769–772
 9. Ohkuma, Y., Sumimoto, H., Horikoshi, M., and Roeder, R.G. (1990) Factors involved in specific transcription by mammalian RNA polymerase II: Purification and characterization of general transcription factor TFIIE. *Proc. Natl. Acad. Sci. USA* **87**, 9163–9167
 10. Ohkuma, Y., Sumimoto, H., Hoffmann, A., Shimasaki, S., Horikoshi, M., and Roeder, R.G. (1991) Structural motifs and potential σ homologies in the large subunit of human general transcription factor TFIIE. *Nature* **354**, 398–401
 11. Sumimoto, H., Ohkuma, Y., Sinn, E., Kato, H., Shimasaki, S., Horikoshi, M., and Roeder, R.G. (1991) Conserved sequence motifs in the small subunit of human general transcription factor TFIIE. *Nature* **354**, 401–404
 12. Peterson, M.G., Inostroza, J., Maxon, M.E., Flores, O., Admon, A., Reinberg, D., and Tjian, R. (1991) Structure and functional properties of human general transcription factor IIE. *Nature* **354**, 369–373
 13. Ohkuma, Y., Hashimoto, S., Wang, C.K., Horikoshi, M., and Roeder, R.G. (1995) Analysis of the Role of TFIIE in basal transcription and TFIIF-mediated carboxy-terminal domain phosphorylation through structure-function studies of TFIIE- α . *Mol. Cell. Biol.* **15**, 4856–4866
 14. Okamoto, T., Yamamoto, S., Watanabe, Y., Ohta, T., Hanaoka, F., Roeder, R.G., and Ohkuma, Y. (1998) Analysis of the role of TFIIE in transcriptional regulation through structure-function studies of the TFIIE subunit. *J. Biol. Chem.* **273**, 19866–19876
 15. Okuda, M., Watanabe, Y., Okamura, H., Hanaoka, F., Ohkuma, Y., and Nishimura, Y. (2000) Structure of the central core domain of TFIIE β with a novel double-stranded DNA-binding surface. *EMBO J.* **19**, 1346–1356
 16. Meinhart, A., Blobel, J., and Cramer, P. (2003) An extended winged helix domain in general transcription factor EIIIE α . *J. Biol. Chem.* **278**, 48267–48274
 17. Okuda, M., Tanaka, A., Arai, Y., Satoh, M., Okamura, H., Nagadoi, A., Hanaoka, F., Ohkuma, Y., and Nishimura, Y. (2004) A novel zinc finger structure in the large subunit of human general transcription factor TFIIE. *J. Biol. Chem.* **279**, 51395–51403
 18. Qian, X., Jeon, C., Yoon, H., Agarwal, K., and Weiss, M.A. (1993) Structure of a new nucleic-acid-binding motif in eukaryotic transcriptional elongation factor TFIIS. *Nature* **365**, 277–279
 19. Qian, X., Gozani, S.N., Yoon, H., Jeon, C., Agarwal, K., and Weiss, M.A. (1993) Novel zinc finger motif in the basal transcriptional machinery: Three-dimensional NMR studies of the nucleic acid binding domain of transcriptional elongation factor TFIIS. *Biochemistry* **32**, 9944–9959
 20. Olmsted, V.K., Awrey, D.E., Koth, C., Shan, X., Morin, P.E., Kazanis, S., Edwards, A.M., and Arrowsmith, C.H. (1998) Yeast transcript elongation factor (TFIIS), structure and function. *J. Biol. Chem.* **273**, 22589–22594
 21. Zhu, W., Zeng, Q., Colangelo, C.M., Lewis, L.M., Summers, M.F., and Scott, R.A. (1996) The N-terminal domain of TFIIB from *Pyrococcus furiosus* forms a zinc ribbon. *Nat. Struct. Biol.* **3**, 122–124
 22. Chen, H.T., Legault, P., Glushka, J., Omichinski, J.G., and Scott, R.A. (2000) Structure of a (Cys3His) zinc ribbon, a ubiquitous motif in archaeal and eucaryal transcription. *Protein Sci.* **9**, 1743–1752
 23. Wang, B., Jones, D.N., Kaine, B.P., and Weiss, M.A. (1998) High-resolution structure of an archaeal zinc ribbon defines a general architectural motif in eukaryotic RNA polymerases. *Structure* **6**, 555–569
 24. Cramer, P., Bushnell, D.A., and Kornberg, R.D. (2001) Structural basis of transcription: RNA polymerase II at 2.8 angstrom resolution. *Science* **292**, 1863–1876
 25. Yang, J.T., Wu, C.C., and Martinez, H.M. (1986) Calculation of protein conformation from circular dichroism in *Methods in Enzymology* (eds. C.W. Hirs and S.N. Timasheff), Vol. 130, pp 208–269, Academic Press, San Diego
 26. Delaglio, F., Grzesiek, S., Vuister, G.W., Zhu, G., Pfeifer, J., and Bax, A. (1995) NMRPipe: A multidimensional spectral processing system based on UNIX pipes. *J. Biomol. NMR* **6**, 277–293
 27. Garrett, D.S., Powers, R., Gronenborn, A.M., and Clore, G.M. (1991) A common sense approach to peak picking in two-, three-, and four-dimensional spectra using automatic computer analysis of contour diagrams. *J. Magn. Reson.* **95**, 214–220
 28. Johnson, B.A., and Blevins, R.A. (1994) NMRView: a computer program for the visualization and analysis of NMR data. *J. Biomol. NMR* **4**, 603–614
 29. Kuldell, N.H., and Buratowski, S. (1997) Genetic analysis of the large subunit of yeast transcription factor IIE reveals two regions with distinct functions. *Mol. Cell. Biol.* **17**, 5288–5298
 30. Maxon, M.E., and Tjian, R. (1994) Transcriptional activity of transcription factor IIE is dependent on zinc binding. *Proc. Natl. Acad. Sci. USA* **91**, 9529–9533
 31. Tjjerina, P., and Sayre, M.H. (1998) A debilitating mutation in transcription factor IIE with differential effects on gene expression in Yeast. *J. Biol. Chem.* **273**, 1107–1113
 32. Yokomori, K., Verruzer, C.P., and Tjian, R. (1998) An interplay between TATA box-binding protein and transcription factors IIE and IIA modulates DNA binding and transcription. *Proc. Natl. Acad. Sci. USA* **95**, 6722–6727
 33. Mullem, V.V., Wery, M., Werner, M., Vandenhoute, J., and Thuriaux, P. (2002) The Rpb9 subunit of RNA polymerase II binds transcription factor TFIIE and interferes with the SAGA and elongator histone acetyltransferases. *J. Biol. Chem.* **277**, 10220–10225
 34. Ghosh, M., Elsby, L.M., Mal, T.K., Gooding, J.M., Roberts, S.G.E., and Ikura, M. (2004) Probing Zn²⁺-binding effects on the zinc-ribbon domain of human general transcription factor TFIIB. *Biochem. J.* **378**, 317–324
 35. Koradi, R., Billeter, M., and Wüthrich, K. (1996) MOLMOL: A program for display and analysis of macromolecular structures. *J. Mol. Graphics* **14**, 51–55